
# INFLUENCE OF PH ON THE TRANSPORT OF SILVER NANOPARTICLES IN SATURATED POROUS MEDIA: LABORATORY EXPERIMENTS AND MODELING

THESIS

Jason R. Flory, Captain, USAF

AFIT/GIH/ENV/12-M02

**DEPARTMENT OF THE AIR FORCE**
**AIR UNIVERSITY**

***AIR FORCE INSTITUTE OF TECHNOLOGY***

**Wright-Patterson Air Force Base, Ohio**

AFIT/GIH/ENV/12-M02

# INFLUENCE OF PH ON THE TRANSPORT OF SILVER NANOPARTICLES IN SATURATED POROUS MEDIA: LABORATORY EXPERIMENTS AND MODELING

THESIS

Presented to the Faculty

Department of Systems and Engineering Management

Graduate School of Engineering and Management

Air Force Institute of Technology

Air University

Air Education and Training Command

In Partial Fulfillment of the Requirements for the

Degree of Master of Science in Industrial Hygiene

Jason R. Flory, BS

Captain, USAF

March 2012

AFIT/GIH/ENV/12-M02

# INFLUENCE OF PH ON THE TRANSPORT OF SILVER NANOPARTICLES IN SATURATED POROUS MEDIA: LABORATORY EXPERIMENTS AND MODELING

Jason R. Flory, BS
Captain, USAF

Approved:

| | |
|---|---|
| _____//signed//_____<br>LEEANN RACZ, Maj, USAF, BSC, PhD, PE (Chairman) | _8 March 2012_<br>Date |
| _____//signed//_____<br>DIRK P. YAMAMOTO, Lt Col, USAF, BSC, PhD, CIH, PE (Member) | _8 March 2012_<br>Date |
| _____//signed//_____<br>MARK GOLTZ, PhD (Member) | _8 March 2012_<br>Date |
| _____//signed//_____<br>SUSHIL KANEL, PhD (Member) | _9 March 2012_<br>Date |

**Abstract**

Given the ubiquity of silver nanoparticles **(**AgNPs), the largest and fastest growing category of nanomaterials, and their potential for toxic effects to both humans and the environment, it is important to understand their environmental fate and transport. The purpose of this study is to gain information on the transport properties of unmodified AgNP suspensions in a glass bead-packed column under saturated flow conditions at different solution pH levels. Commercial AgNPs were characterized using high resolution transmission spectroscopy (HRTEM), dynamic light scattering (DLS) and ultraviolet (UV) visible spectroscopy. Transport data were collected at different pH levels (4, 6.5, 9 and 11) at fixed ionic strength. Capture of AgNPs increased as the pH of the solution increased from 4 to 6.5. Further increase in pH to 9 and 11 decreased the attachment of AgNPs to the glass beads. AgNP concentration versus time breakthrough data were simulated using an advection-dispersion model incorporating both irreversible and reversible attachment. In particular, a reversible attachment model is required to simulate breakthrough curve tailing at near neutral pH, when attachment is most significant.

## Table of Contents

Page

## List of Figures

## List of Tables

## List of Equations

# INFLUENCE OF PH ON THE TRANSPORT OF SILVER NANOPARTICLES IN SATURATED POROUS MEDIA: LABORATORY EXPERIMENTS AND MODELING

## I. Introduction

### Silver NP Applications

Because of the antimicrobial properties and electrical conductivity of silver nanoparticles (NPs), these materials are being applied to a wide variety of fields, including biomedical, chemical and electrical engineering. Colloidal nanosilver has been used as a medication for nearly one hundred years (Nowack et al. 2011). The combination of their antimicrobial activity and relatively low cost is likely an important reason for nanosilver-containing products to comprise more than 50% of consumer products that contain engineered nanoparticles as of 2011 (Huynh and Chen 2011). Silver nanoparticles are being incorporated into the manufacture of clothes, bandages and food containers as deodorizers and disinfectants. Studies have been conducted that explore the potential use of silver nanoparticles in drinking water treatment (Huynh and Chen 2011). Silver compounds were a key weapon against wound infection during World War I, until the advent of antibiotics (Chen and Schluesener 2008). Nanosilver is an effective killer of a broad range of Gram-negative and Gram-positive bacteria, including antibiotic-resistant strains (Wijnhoven et al. 2009). Nanosilver is a successful fungicide against common fungi, such as *Aspergillus, Candida* and *Saccharomyces*, and it also inhibits HIV-1 virus replication and formation of biofilms (Wijnhoven et al. 2009).

For these reasons, military-specific applications of nanosilver might include uniform textiles and wound dressings.

**Silver NPs in the Environment**

Not all silver nanoparticles are engineered or man-made. Silver in natural waters is typically associated with the particulate and colloidal forms and is therefore to some extent naturally present as nanoparticles and metal-sulfide clusters (Nowack et al. 2011). There is no conventional treatment that can definitively protect consumers from exposure to waterborne nanoparticles, either through recreational use or drinking water consumption (Weinberg et al. 2011). Furthermore, most common analytical equipment is unable to accurately characterize nanosilver suspensions at the lower range of toxicologically relevant concentrations that would be expected in an environmental release (<< 1 mg/L) (Kennedy et al. 2010).

Many aspects of nanosilver behavior, including antibacterial potency, eukaryotic toxicity, environmental release and particle persistence, are influenced by the ionic activity of the particle suspension (Liu and Hurt 2010). Ion release rates increase with temperature in the range 0-37°C and decrease with increasing pH or addition of humic or fulvic acids (Liu and Hurt 2010). Colloids of spherical AgNPs have a characteristic yellow color due to their surface plasmon absorption near 400 nm (Amendola et al. 2007), although suspensions of nanosilver in varying ionic strength solutions have been observed with colors such as orange, red, blue and gray (Kennedy et al. 2010).

Ionic silver ($Ag^+$) can adsorb to nanosilver particles, so high particle concentrations would provide more binding surfaces for $Ag^+$ (Kennedy et al. 2010). Since $Ag^+$ adsorbs to silver nanoparticle surfaces, even simple colloids contain three forms of silver: $Ag^0$ solids, free $Ag^+$ (or its compounds) and surface-adsorbed $Ag^+$ (Liu and Hurt 2010). In Liu and Hurt (2010), both thermodynamic analysis and kinetic measurements indicated that $Ag^0$ nanoparticles would not be persistent in environments containing dissolved oxygen, but would be converted to the ion form by reactive dissolution. In addition, natural organic matter, which is common in natural waters, has been shown to adsorb to the surface of nanoparticles, enhancing their stability through either steric or electrostatic repulsion (Li et al. 2010).

Most synthesis methods fabricate silver nanoparticles that are spherical with a diameter of less than 20 nm (Tolaymat et al. 2010). The synthesis procedures are categorized into top-down and bottom-up methods (Tolaymat et al. 2010). The top-down techniques take silver in bulk form and mechanically reduce its size to the nanoscale using specialized methods such as lithography or laser ablation. The bottom-up (also known as self-assembly) technique involves dissolution of silver salt, such as silver nitrate, into a solvent, followed by addition of a reducing agent (e.g., $NaBH_4$), possibly supplemented by a stabilizing agent, like citrate, to prevent agglomeration of nanoparticles (Tolaymat et al. 2010). The specific solvents and reducing agents used in these processes affect the physical characteristics of the resulting manufactured silver nanoparticles. These specific characteristics, in turn, influence the fate, transport and toxicity of these nanoparticles in the environment. For example, sodium citrate used as a

reducing agent generates a negatively charged nanoparticle, which may behave differently than a positively charged nanoparticle generated using branched polyethyleneimine (Tolaymat et al. 2010).

As silver nanoparticle production increases, so do concerns about potential adverse effects on human health and the environment. Many products that make use of silver nanoparticles may release silver in the form of nanoparticles or soluble ions during use, washing, abrasion or disposal (Liu et al. 2010). Modeling results indicate that up to 15% of total silver in the form of ions or AgNPs could be released from antibacterial plastics and textiles into water (Choi et al. 2009), and a study by Benn and Westerhoff (2008) found that half of the socks studied released nearly 100% of their silver content in four consecutive washes. Silver nanoparticles themselves can act as a slow-release source of ionic silver over time (Tolaymat et al. 2010), though the dissolution process is dependent on environmental conditions, such as pH.

The growing use of nanosilver in food products, medical applications, sprays and other consumer products and the increasing use and disposal of nanosilver in the environment imply that human exposure to nanosilver is inevitable and that this exposure can be expected to increase in the near future (Wijnhoven et al. 2009).

**Toxicity**

Silver nanoparticles are a broad-spectrum antimicrobial agent that act on more than 650 different types of disease-causing organisms, including viruses (Schrand et al.

2010). Three mechanisms have been proposed for the antimicrobial properties of silver nanoparticles (Tolaymat et al. 2010):

1. adhesion of nanoparticles to the bacterial surface, altering membrane properties, with possible degradation of lipopolysaccharide molecules and accumulation inside the membrane by forming pits and causing large increases in membrane permeability
2. penetration of silver nanoparticles inside the bacterial cell, resulting in DNA damage
3. dissolution of silver nanoparticles, with releases of antimicrobial ionic silver

Eukaryotic (mammalian) cells appear less sensitive to silver, which may be explained by the higher structural and functional redundancy and size of eukaryotic compared to prokaryotic (bacterial) cells (Wijnhoven et al. 2009). This difference may result in an increase in the silver concentration needed to achieve comparable toxic effects on eukaryotic cells versus bacterial cells.

As the size of a particle shrinks, its surface-area-to-volume ratio increases, allowing a higher proportion of its atoms or molecules to be located on the surface, resulting in increased surface reactivity (Schrand et al. 2010). As particle size decreases, there is a propensity for toxicity to increase, even if the same material is relatively harmless in bulk form. Nanoparticles may be able to enter the body via routes such as the gastrointestinal tract, lungs, injection into the blood stream and passage through the skin (Schrand et al. 2010). Silver and copper nanoparticles have shown a greater potential to

migrate through organ systems, compared to larger materials, and may not be detected by normal phagocytic defenses, allowing the particles to gain access to the bloodstream or cross the blood–brain barrier into the nervous system (Schrand et al. 2010).

Although some uncertainty remains about the precise mechanism(s) of nanosilver toxicity, one potential explanation is the interaction of nanoparticles with microbes, involving silver ion release and particle cellular internalization (Choi et al. 2010). Others have postulated a contribution from particle surface reactions that either generate reactive oxygen species (ROS), leading to oxidative stress, or catalyze oxidation of cellular components (Liu et al. 2010). ROS are considered to be the major source of spontaneous damage to DNA (AshaRani et al. 2009). Silver nanoparticles or silver ions inside the cell nucleus may bind to DNA and enhance the DNA damage caused by ROS (AshaRani et al. 2009). DNA-damaging agents have the potential to cause genome instability, which is a predisposing factor in carcinogenesis (AshaRani et al. 2009). The generation of ROS can oxidize double bonds on fatty acid tails of membrane phospholipids in a process known as lipid peroxidation, which increases membrane permeability and fluidity, making cells more susceptible to osmotic stress and impeding nutrient uptake (Klaine et al. 2008). Peroxidized fatty acids can then elicit reactions that create other free radicals, leading to further cell membrane and DNA damage.

Silver nanoparticles can also be seen as ionic delivery agents, where nanosilver acts in an analogous fashion to a drug delivery system in which the nanoparticle contains a concentrated inventory of silver ions, which is transported to and released at or near biological target sites (Liu et al. 2010). Thiol-containing proteins have been shown to be

major targets for silver ion toxicity; thiols in living systems play an important role in antioxidant defense, protein synthesis and structure and immune regulation (Liu et al. 2010). Ionic silver may, in turn, bind to sulfur- and phosphorus-containing molecules (e.g., S-adenosylmethionine, cysteine, taurine, glutathione) involved in cell antioxidant defense and may thereby result in a drop in the intracellular concentration of these molecules. The toxicity of AgNPs is also derived, in part, from their effect on cellular energy metabolism, as AgNPs have been shown to decrease mitochondrial function (Kim et al. 2009). Potential target organs of nanosilver may include the liver and the immune system (Wijnhoven et al. 2009).

Nanosilver toxicity is also species-specific (Choi et al. 2010). Ionic silver is considered to be the second most toxic metal, after mercury, to freshwater fish and invertebrates (Kennedy et al. 2010). In a study of the effects of nanosilver on fish, Shaw and Handy (2011) found an increase in hepatic silver that indicates there was some uptake and transport of silver from nanoparticles themselves, which cannot be explained by dissolution of silver ions alone. Unusual pathologies due to nanoparticles observed in the brain of fish and elsewhere also suggest there may be additional or unique hazards attributable to the nanoscale (Shaw and Handy 2011). Another study by Kennedy et al. (2010) indicated a trend of decreasing toxicity with increasing particle size.

Furthermore, in a study by Kim et al. (2008) on rats, 28 days of repeated oral doses of silver nanoparticles induced liver toxicity and demonstrated a coagulation effect on peripheral blood. The kidneys showed a sex-dependent accumulation of silver, with a

twofold higher accumulation in female rats when compared with male rats across all dose groups (Kim et al. 2008).

**Effects of Environmental Conditions on NP Transport**

The fact that groundwater is a critical pathway by which contaminants have potential to reach biological receptors, including humans, makes the fate and transport of nanosilver in groundwater a concern. The fate and transport of silver nanoparticles are controlled by many variables, such as whether the particles have a capping agent, particle size and surrounding environmental conditions (Tolaymat et al. 2010). Bacterially-produced proteins play a role in the aggregation of natural nanoparticles and the aggregation state of nanoparticles may affect their transport in the environment, as well as their chemical reactivity (Aruguete and Hochella 2010). The stability of nanoparticles is an area of current research, but it is clear that in many cases nanoparticle suspensions can be stable in the environment, especially in the presence of organic solutes that associate with colloid surfaces (Nelson and Ginn 2011). Because of this environmental stability, it is important to develop an understanding of the fate and transport of environmental nanosilver. The movement of nanoparticles in porous media is impeded by two processes: (1) straining or physical filtration, where a particle is larger than the pore and is trapped and (2) filtration where the particle is removed from solution by interception, diffusion and sedimentation (Nowack and Bucheli 2007); however, particles removed from solution by these processes can easily become re-suspended when changes occur in chemical or physical conditions (e.g., changes in pH, ionic strength, flow rate).

Ionic strength and pH are two environmental parameters that have been observed to influence nanoparticle behavior in water (Johnson et al. 2007). According to Navarro et al. (2008), an increase in ionic strength compresses the electric double layer, thus decreasing electrostatic repulsion between two objects with the same charge; the energy barrier then decreases and the attachment probability increases. El Badawy et al. (2010) found that uncoated and citrate- and $NaBH_4$-coated silver nanoparticles aggregated at higher ionic strengths (100 mM $NaNO_3$) and/or acidic pH (3.0), while the presence of $Ca^{2+}$ (10 mM) resulted in aggregation of the silver nanoparticles without regard to pH. The surface charge and aggregation of branched polyethylenimine-coated silver nanoparticles also varied according to solution pH (El Badawy et al. 2010). Li et al. (2010) found that increasing electrolyte concentration leads to a corresponding increase in aggregation rate by diminishing the electrostatic energy barrier to aggregation that exists between negatively charged AgNPs (Li et al. 2010). In a study of titania ($TiO_2$) nanoparticles, the deposition process, a retention mechanism of nano-$TiO_2$ in saturated porous media, was impacted by surfactant and pH (Godinez et al. 2011). Surfactants are commonly used to enhance nanoparticle stability or dispersion in solution.

In a study by Tian et al. (2010), sodium dodecylbenzene sulfonate, an anionic surfactant, was used to disperse engineered nanoparticles, enhancing their stability in water; the solubilized nanoparticles were then applied to laboratory columns packed with two types of water-saturated quartz sand to obtain their effluent concentration versus time breakthrough curves. The experimental results showed the surfactant-solubilized nanoparticles were highly mobile in saturated porous media; less than 15% of the silver

nanoparticles were retained in the column during the breakthrough experiments (Tian et al. 2010). The Derjaguin–Landau–Verwey–Overbeek (DLVO) theory and a colloid transport model were used to simulate the fate and transport of the engineered nanoparticles in the sand columns; the DLVO theory worked well in modeling transport of the silver nanoparticles (Tian et al. 2010). However, in similar column experiments by Lin et al. (2011), DLVO theory alone was not sufficient to predict attachment efficiency of AgNP.

DLVO theory was also unsuccessful in predicting transport of zerovalent iron nanoparticles in a study by Lerner et al. (2012), in which a model that incorporated steric effects as well as DLVO effects was necessary to adequately describe the particle retention seen in column experiments. Attachment of nanoparticles in porous media is the result of a combination of forces, including van der Waals attraction, steric interactions, hydrophobic interactions and electrostatic repulsions (Lerner et al. 2012). For example, increased surface charge has been shown to increase inter-particle repulsion and nanoparticle mobility in saturated porous media (Petosa et al. 2012).

Engineered nanoparticles released into the environment are typically coated with natural or engineered organic materials, which are known to considerably influence the attachment of nanoparticles to porous media. Song et al. (2011) explored the effects of several different coatings on transport through glass beads. They found that coatings with higher hydrophobicity have greater attachment to hydrophobic surfaces, but attachment efficiencies are low overall, due to the repulsive interactions between AgNPs and glass beads, both of which have a net negative surface potential (Song et al. 2011).

Soil characteristics are also thought to have an effect on AgNP transport. Transport through a negatively charged sandy soil will be dominated by repulsion forces, causing AgNPs to be more mobile, while transport through positively charged soils will be dominated by attraction forces, deterring AgNPs from reaching groundwater (Tolaymat et al. 2010).

**Problem Statement**

Current literature lacks a thorough examination of the effect of solution pH on AgNP fate and transport. Lin et al. (2011) investigated the effect of ionic strength on AgNP transport, and some of their work has been duplicated and confirmed in this present study, but the purpose of Lin et al. was to examine the effect of porous media surface composition, so only two pH values were studied. The present study aims to advance the state of AgNP research by more thoroughly investigating the effect of pH on attachment efficiency and incorporating findings into a useful model.

**Research Objectives**

The objective of this study is to investigate how AgNPs are transported in groundwater under different pH conditions. Specific questions to be answered include:

1. What physical and chemical processes (advection, dispersion, filtration, aggregation, release of $Ag^{+}$) are relevant to transport of AgNPs in porous media?
2. What model governing equations and parameter values are appropriate to describe AgNP fate and transport in porous media?

3. How is AgNP transport affected by the presence of hydrogen ions in groundwater?
4. How do the model governing equations and parameter values change in response to the presence of hydrogen ions in groundwater?

**Scope and Approach**

Glass columns, fitted with tubing and packed with glass beads, were constructed, into which a peristaltic pump was used to feed background solution of Cl ion and suspensions of AgNPs. The quantification of AgNP particles in suspensions at different pH levels before and after passing through the porous media-packed column was performed using analytical methods such as high resolution transmission spectroscopy (HRTEM), dynamic light scattering (DLS) and ultraviolet (UV) visible spectroscopy. The zeta-potential and particle size distribution of AgNPs were measured at 25°C, at different pH levels, using zeta sizing and DLS.

Experimental results were analyzed using a mathematical model that describes the processes affecting the fate and transport of nanomaterials (NMs) in porous media. Based on results obtained at various pH levels, parameters that provide the best fit of model simulation to the data were obtained.

**Significance**

Due to the rapidly expanding quantity of NMs that are manufactured, transported, used and disposed of in society, it is inevitable that releases into the environment (both

intentional and accidental) will be common. Many of these releases will occur on the ground surface and subsurface and it is possible that significant quantities of NMs will make their way to groundwater, where they will be transported to human and environmental receptors downstream. Clarification of the various transport processes will provide fuller understanding of the risks posed by intentional or accidental releases of nanosilver into the subsurface and enable better decision-making to manage those releases.

**Preview**

This thesis uses the scholarly article format. Chapter II contains the journal article which will be submitted to *Environmental Science and Technology*. As an independent chapter, the article includes the abstract, introduction, materials and methods, and results and discussion of this research as prescribed by the selected journal. Chapter III provides a summary of the primary findings discussed in the article, as well as related topics for future study.

## II. Scholarly Article

### Influence of pH on the transport of silver nanoparticles in saturated porous media: Laboratory experiments and modeling

Jason Flory, Sushil R. Kanel, LeeAnn Racz, Christopher Impeliteri, Rendahandi G. Silva, Mark N. Goltz

**Abstract**

Given the ubiquity of silver nanoparticles **(**AgNPs), the largest and fastest growing category of nanomaterials, and their potential for toxic effects to both humans and the environment, it is important to understand their environmental fate and transport. The purpose of this study is to gain information on the transport properties of unmodified AgNP suspensions in a glass bead-packed column under saturated flow conditions at different solution pH levels. Commercial AgNPs were characterized using high resolution transmission spectroscopy (HRTEM), dynamic light scattering (DLS) and ultraviolet (UV) visible spectroscopy. Transport data were collected at different pH levels (4, 6.5, 9 and 11) at fixed ionic strength. Capture of AgNPs increased as the pH of the solution increased from 4 to 6.5. Further increase in pH to 9 and 11 decreased the attachment of AgNPs to the glass beads. AgNP concentration versus time breakthrough data were simulated using an advection-dispersion model incorporating both irreversible and reversible attachment. In particular, a reversible attachment model is required to simulate breakthrough curve tailing at near neutral pH, when attachment is most significant.

## Introduction

Engineered metal nanomaterials (NMs) are extensively used in various sectors due to their unique physical and chemical properties that differ from their bulk counterparts (Aitken et al. 2006, Kanel and Al-Abed 2011). Silver nanoparticles (AgNPs) have become one of the most widely used nanomaterials in consumer products (Impellitteri et al. 2009, Benn et al. 2010), medical and pharmaceutical supplies (Faunce and Watal 2010), environmental applications and electronics (Kim et al. 2007, Wijnhoven et al. 2009, Tolaymat et al. 2010). The extensive use of AgNPs is largely due to their potency as broad-spectrum antimicrobial and antiviral agents (Kim et al. 2007). The United States Environmental Protection Agency (USEPA) has set water quality criteria values for silver in fresh water and salt water at 3.2 $\mu gL^{-1}$ and 1.9 $\mu gL^{-1}$, respectively (USEPA 2012). The USEPA has also instituted a secondary drinking water standard for silver of 100 $\mu gL^{-1}$ (Benn and Westerhoff 2008). Even though there is no maximum contaminant level for silver or AgNPs, recently, USEPA has categorized NMs as emerging contaminants, specifically noting the potential toxic effects of AgNPs (USEPA 2010).

Recent *in vitro* and *in vivo* studies using various cell lines, algae, zooplankton, fish, rats and mice have indicated that AgNPs have toxic effects (Nel et al. 2006, Yang et al. 2010). Due to the inevitable release of AgNPs into the environment, their fate and transport need to be investigated. In particular, understanding is needed as to how AgNPs are transported in the subsurface by groundwater, as groundwater is an important pathway of contaminants to human and environmental receptors (Fan et al. 2010).

A limited number of batch and column studies have been conducted using AgNPs to better understand their behavior under various environmental conditions. The surface charge and hydrodynamic diameter of AgNPs in batch experiments were investigated for different pH values, ionic strengths and background electrolytes (El Badawy et al. 2011). The investigators found that the size of sodium borohydride-reduced AgNPs in batch experiments were 13 nm, 14 nm and 12 nm in 10 mM NaCl solution at pH of 3, 6 and 9, respectively. Batch study showed AgNPs turn to $Ag_2S$ in the presence of sulfur and chainlike structures form (Levard et al. 2011). The influence of dissolved oxygen on aggregation kinetics of citrate-coated AgNPs in a batch study has been reported (Zhang et al. 2011). The studies reported above were based on batch experiments. However, to better understand AgNP transport in groundwater, column experiments are more useful (Kanel et al. 2008, Kanel and Al-Abed 2011).

There are limited studies reported on AgNP transport through porous media in column studies for example sodium dodecylbenzene sulfonate (SDBS)-stabilized silver oxide-coated AgNPs were studied in column experiments. There was incomplete breakthrough of AgNPs (AgNP peak effluent concentrations were 80% of the influent concentration) and nearly 15% of the AgNPs were retained in the saturated column (Tian et al. 2010). Interaction of gum arabic- (GA), citrate- and polyvinylpyrrolidone (PVP)-coated AgNPs with hydrophobic (octadecylichlorosilane (OTS)-coated glass beads) and hydrophilic (glass bead) surfaces was investigated in column experiments at pH 8.1 (Song et al. 2011). The authors found that the attachment efficiencies of GA- and PVP-coated AgNPs increased two- and four-fold, respectively, in OTS-coated glass beads,

compared to clean glass beads. Citrate-coated AgNPs showed no substantial change in attachment efficiency between hydrophobic and hydrophilic collector surfaces (Song et al. 2011). The transport of uncoated AgNPs in porous media (glass beads and hematite-coated glass beads) at acidic and basic pH was studied in column experiments. At pH levels lower than the point of zero charge of hematite, the affinity of AgNPs for hematite-coated glass bead surfaces was significantly higher than that for uncoated surfaces. Lin et al. (2011) studied the adsorption of unpurified AgNPs in hematite-coated and uncoated glass bead-packed columns, but the desorption of AgNPs from glass bead-packed columns was not studied. As AgNPs are released into the environment, they encounter soil and groundwater at differing pH levels. Hence, there is a need for conducting column experiments to study AgNP fate and transport in subsurface environments over a broad range of pH levels and capture the adsorption and desorption patterns of AgNP.

Sodium dodecylbenzene sulfonate (SDBS)-stabilized silver oxide-coated AgNPs were studied in column experiments by Tian et al. (2010). In that study, there was incomplete breakthrough of AgNPs (AgNP peak effluent concentrations were 80% of the influent concentration) and nearly 15% of the AgNPs were retained in the saturated column. The Tian et al. study was conducted at a single, fixed pH, as was a study by Song et al. (2011) that examined stabilized AgNP transport through surface-modified and pristine glass bead-packed columns at pH 8.1. As AgNPs are released into the environment, they encounter soil and groundwater at differing pH levels. Hence, there is a need for column experiments that study AgNP fate and transport in subsurface environments over a broad range of pH levels. Such a study was accomplished by Lin et

al. (2011), which investigated transport of uncoated AgNPs in porous media (glass beads and hematite-coated glass beads) at acidic and basic pH. At pH levels lower than the point of zero charge of hematite, the affinity of AgNPs for hematite-coated glass bead surfaces was significantly higher than that for uncoated surfaces (Lin et al. 2011). While Lin et al. examined the adsorption of unpurified AgNPs in hematite-coated and uncoated glass bead-packed columns, the desorption of AgNPs from glass bead-packed columns was not studied, an issue which is addressed by this present study.

The goal of this study is to investigate how AgNPs at different pH are transported through porous media consisting of one-dimensional columns filled with glass beads. AgNPs were input as a continuous source at the influent end of a column to observe attachment, followed by a continuous source of 0.01 mM KCl to observe detachment of AgNPs from the media. We then model AgNP transport by simulating concentration versus time breakthrough data at the column outlet using an advection-dispersion equation, modified to account for AgNP attachment to and detachment from the glass beads.

## Materials and Methods

### *Materials*

Approximately 1000 $mgL^{-1}$ concentration of AgNPs (99.99% pure) was purchased from US Research Nanomaterials, Inc. (Houston, TX). The density of AgNPs was 10.5 $g/cm^3$. NaOH and $HNO_3$ were purchased from Sigma-Aldrich. All reagents

were used as received without further purification. Ultra-pure water (Millipore, 18.2 MΩ-cm) was used to prepare all solutions.

***Column Experiments***

A glass column (2.5 cm inner diameter × 5 cm length, Cluxton Instruments) having an empty bed volume of 24.5 $cm^3$ was used in all experiments. The Teflon tubing (PTFE, 2 mm OD, Cluxton Instruments) connected to the column was soaked overnight in 0.1 M aqueous $HNO_3$ solution and rinsed with deionized water to remove silver from the tubing. The column was packed for each experiment with 45.0 g of fresh porous material (glass beads of 425 to 600 μm diameter, Sigma-Aldrich) with the intent of preventing cross-contamination between experiments, although some variation in packing density or media porosity may have been introduced by re-packing the column for each experiment. The glass beads were not perfectly homogeneous, with defects of about 50 nm in size, and separated from each other at a distance of about 0 to 200 nm (Figure 1). A peristaltic pump (0−100 rpm, MasterFlex) was used to feed 0.01 mM KCl background solution for 60 minutes in each experiment before passing either tracer solution (60 mL of 3 mM aqueous KCl solution) or colloidal AgNPs (60 mL of 15 $mgL^{-1}$ colloidal silver) into the column for 60 minutes as reported in our previous work (Kanel and Choi 2007, Kanel et al. 2007, Kanel and Al-Abed 2011). The influent solution flow rate (1 $mLmin^{-1}$) was measured beforehand and continuously monitored to ensure a constant flow rate. An upward flow direction was maintained to equilibrate the porous material with the influent solution and to enhance packing homogeneity. Glass wool (0.1 g) was placed at both ends of the column to prevent elution of the porous material. The effluent was collected

for silver content analysis by inductively coupled plasma optical emission spectrometry (ICP-OES). After achieving breakthrough of KCl tracer or AgNPs, background solution was passed through the column for 120 minutes. All column experiments were performed in duplicate and average values are reported. In each experiment, 90 effluent samples were taken. The average difference between duplicates for all 90 samples was less than 5%, although several duplicates differed by as much as 20%.

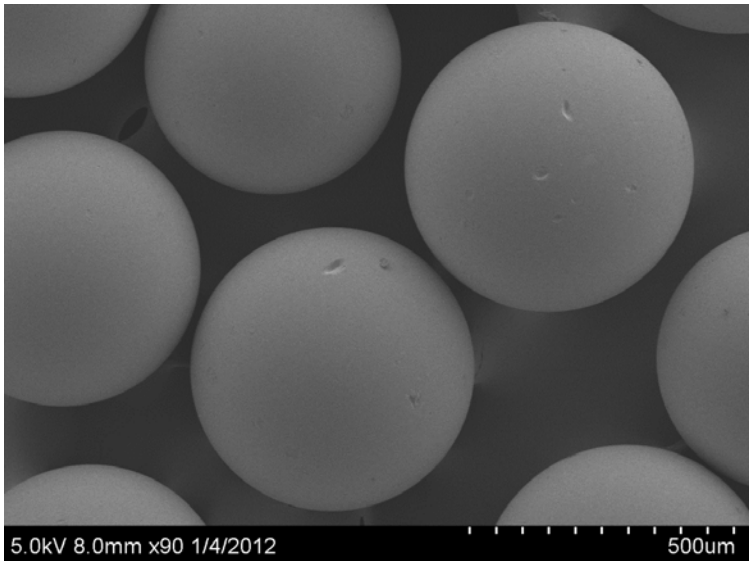


**Figure 1: SEM image of glass beads**

***Instrumentation and Analysis***

The UV absorbance of the AgNP suspensions was measured by UV-vis spectrophotometer (UV-Cary 60, Agilent). An absorbance peak for AgNPs was observed at 410 nm, close to that found in the literature (Lin et al. 2011). Influent stock solutions and column effluent samples were diluted to an effective acid concentration of 5% $HNO_3$, and then analyzed by ICP-OES. The efficacy of this sample preparation procedure was

verified by EPA Method 3015, followed by ICP-OES analysis. The hydrodynamic diameter (HDD) of AgNPs was measured by dynamic light scattering (DLS) using a Zetasizer Nanoseries (Malvern Instruments) with a 633 nm laser source and a detection angle of 173° (HDD detection range 0.3 nm to 10 μm). The Zetasizer was also used to measure electrophoretic mobility, which was converted to zeta potential using Smoluchowski's approximation (see Song et al. 2011, El Badawy et al. 2010, Liu et al. 2009). HRTEM was used to measure the shape and size of AgNPs.

***Modeling***

We developed a model to help better describe and understand AgNP transport in porous media. The model incorporates the processes of advection and dispersion to describe transport in a porous medium. AgNP attachment was simulated as either irreversible (Equation 1)

$$\frac{\partial N}{\partial t} = D\frac{\partial^2 N}{\partial x^2} - v\frac{\partial N}{\partial x} - \lambda N \qquad \text{Eq. 1}$$

or as both an irreversible and a rate-limited reversible process (Equations 2 and 3).

$$\theta\frac{\partial N}{\partial t} + \rho\frac{\partial N_s}{\partial t} = D\theta\frac{\partial^2 N}{\partial x^2} - v\theta\frac{\partial N}{\partial x} - \lambda\theta N \qquad \text{Eq. 2}$$

$$\frac{\partial N_s}{\partial t} = \alpha\left(\frac{k_f}{\alpha}N - N_s\right) \qquad \text{Eq. 3}$$

where $N$ and $N_s$ are the concentrations of aqueous and attached nanoparticles, respectively, $\rho$ is the bulk density of the porous medium, $\theta$ is the porosity of the porous medium, $D$ is a dispersion coefficient, $v$ is the average pore velocity of the water, $t$ is time, $x$ is length, $\lambda$ is a first-order irreversible attachment rate constant, and $k_f$ and $\alpha$ are

first-order attachment/detachment rate constants, respectively. For a clean one-dimensional column with a finite-pulse third type boundary condition at the inlet, the initial and boundary conditions are:

$$N(x,t=0) = N_s(x,t=0) = 0 \qquad \text{Eq. 4a}$$

$$\begin{aligned}(vN - D\frac{\partial N}{\partial x})\big|_{x=0} &= vN_0 \qquad 0 < t < t_p \\ &= 0 \qquad\quad t > t_p\end{aligned} \qquad \text{Eq. 4b}$$

$$N(x \to \infty, t) = 0 \qquad \text{Eq. 4c}$$

where nanoparticles at a concentration of $N_0$ are injected into the column inlet ($x = 0$) for a time period $t_p$.

Nondimensional versions of Equations 1 through 4 are

$$\frac{\partial \overline{N}}{\partial T} = \frac{1}{Pe}\frac{\partial^2 \overline{N}}{\partial \overline{x}^2} - \frac{\partial \overline{N}}{\partial \overline{x}} - Da^I_{irrev}\overline{N} \qquad \text{Eq. 5}$$

$$\frac{\partial \overline{N}}{\partial T} + \frac{\partial \overline{N}_s}{\partial T} = \frac{1}{Pe}\frac{\partial^2 \overline{N}}{\partial \overline{x}^2} - \frac{\partial \overline{N}}{\partial \overline{x}} - Da^I_{irrev}\overline{N} \qquad \text{Eq. 6}$$

$$\frac{\partial \overline{N}_s}{\partial T} = Da^I_{rev}(\overline{N} - \overline{N}_s) \qquad \text{Eq. 7}$$

$$\overline{N}(\overline{x}, T=0) = \overline{N}_s(\overline{x}, T=0) = 0 \qquad \text{Eq. 8a}$$

$$\begin{aligned}(\overline{N} - \frac{1}{Pe}\frac{\partial \overline{N}}{\partial \overline{x}})\big|_{\overline{x}=0} &= 1 \qquad 0 < T < T_p \\ &= 0 \qquad\quad T > T_p\end{aligned} \qquad \text{Eq. 8b}$$

$$\overline{N}(\overline{x} \to \infty, T) = 0 \qquad \text{Eq. 8c}$$

where

$T = \frac{vt}{L}$ is a dimensionless time scale, also referred to as pore volume (PV)

$\bar{x} = \frac{x}{L}$ is a dimensionless length scale

$L$ is the length of the column

$\overline{N} = \frac{N}{N_0}$ is a nondimensional aqueous phase nanoparticle concentration

$\overline{N}_s = \frac{N_s}{\frac{k_f}{\alpha} N_0}$ is a nondimensional attached nanoparticle concentration

$Pe = \frac{vL}{D}$ is a Peclet number, the ratio of a dispersion time scale to an advection time scale

$Da^I_{irrev} = \frac{\lambda L}{v}$ is a Damkohler number, the ratio of an advection time scale to an irreversible attachment time scale

$Da^I_{rev} = \frac{\alpha L}{v}$ is also a Damkohler number, in this case the ratio of an advection time scale to a reversible attachment/detachment time scale

$T_p = \frac{vt_p}{L}$ is the dimensionless input pulse time

Solutions presented in a program by Valocchi and Werth (2004) were used to model reversible and irreversible attachment of AgNPs (Valocchi and Werth 2004) (Equations 6 and 7, with boundary and initial conditions 8).

## Results and Discussion

### *Characterization of AgNPs*

The HRTEM images (Figure 2a) show round AgNPs with no aggregation. A size histogram (Figure 2b), prepared by analyzing the TEM images of 500 AgNPs at pH 6.5 (without adding acid or base), indicates an average diameter of 17 nm. The diameters ranged from 9 nm to 30 nm.

Zeta potential and hydrodynamic diameter of AgNPs were measured at pH 3-11. The point of zero charge (PZC) of the AgNPs was not found in the pH range of 3-11. At all pH levels, AgNPs were negatively charged with values ranging from -8 mV to -16 mV (Figure 3), which agrees with the literature. For example, El Badawy et al. (2010) found the zeta potential of sodium borohydride-reduced AgNPs (no surface coating) were approximately -32 mV and -44 mV at pH 3 and pH 11, respectively. The same study also observed zeta potential of uncoated AgNPs becoming less negative at alkaline pH levels of 9 and higher (El Badawy et al. 2010), which this present study confirms. Positive surface charge is not typically seen on AgNP at any pH, unless engineered with a surface coating for this purpose (El Badawy et al. 2010).

The hydrodynamic size of AgNPs ranged from 29 to 38 nm (Figure 3). The reason this size range differs from the observed HRTEM measured size is that DLS gives a hydrodynamic size, rather than a physical size, and DLS has a bias toward larger size fractions (Cumberland and Lead 2009, Khlebtsov and Khlebtsov 2011).

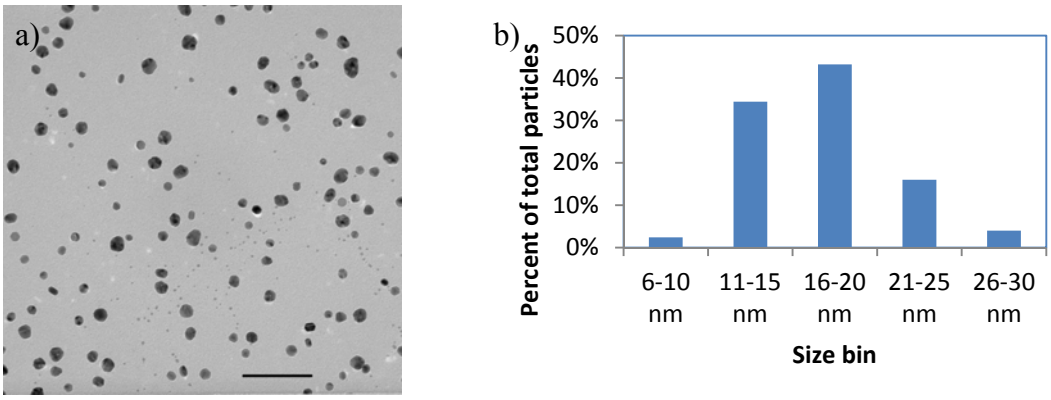


**Figure 2: (a) HRTEM image of AgNP. Scale bar is 100 nm. (b) Size histogram prepared by analysis of HRTEM images of 500 AgNPs.**

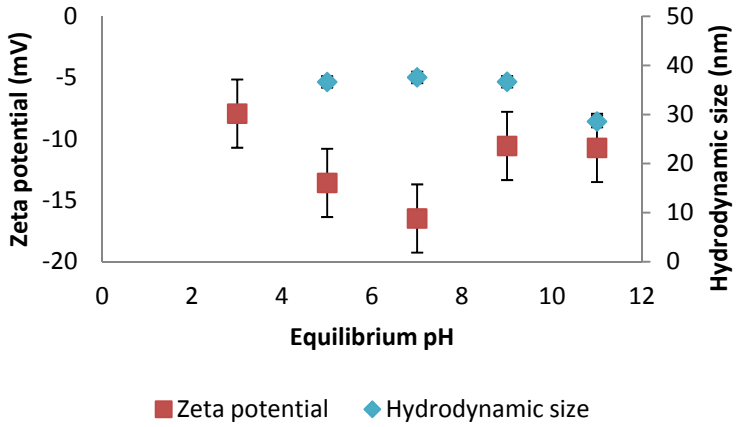


**Figure 3: Zeta potential and hydrodynamic size of AgNP at different pH levels. Experimental conditions: AgNP 15 mg/L, ionic strength 0.01 mM KCl.**

### *Transport of AgNPs*

Figure 4 shows the breakthrough curves (BTCs) which plot the normalized effluent concentration of Cl ion and AgNPs at different pH (4, 6.5, 9 and 11) as a function of pore volume. It was assumed that the Cl tracer achieved breakthrough at 1 pore volume, so a pore volume value was chosen (11.43 mL) that supports this assumption, when compared with tracer effluent sample data. A pore volume of 11.43

mL results in a bed porosity of 0.47, which was used in modeling calculations. The concentration of Cl ion (tracer) in the effluent increased with the continuous injection of the first 3 pore volumes of solution in aqueous phase and reached a stable plateau at $C/C_0 = 1$. AgNPs were retarded by the porous medium and reached a stable plateau at $C/C_0 < 1$ at each pH.

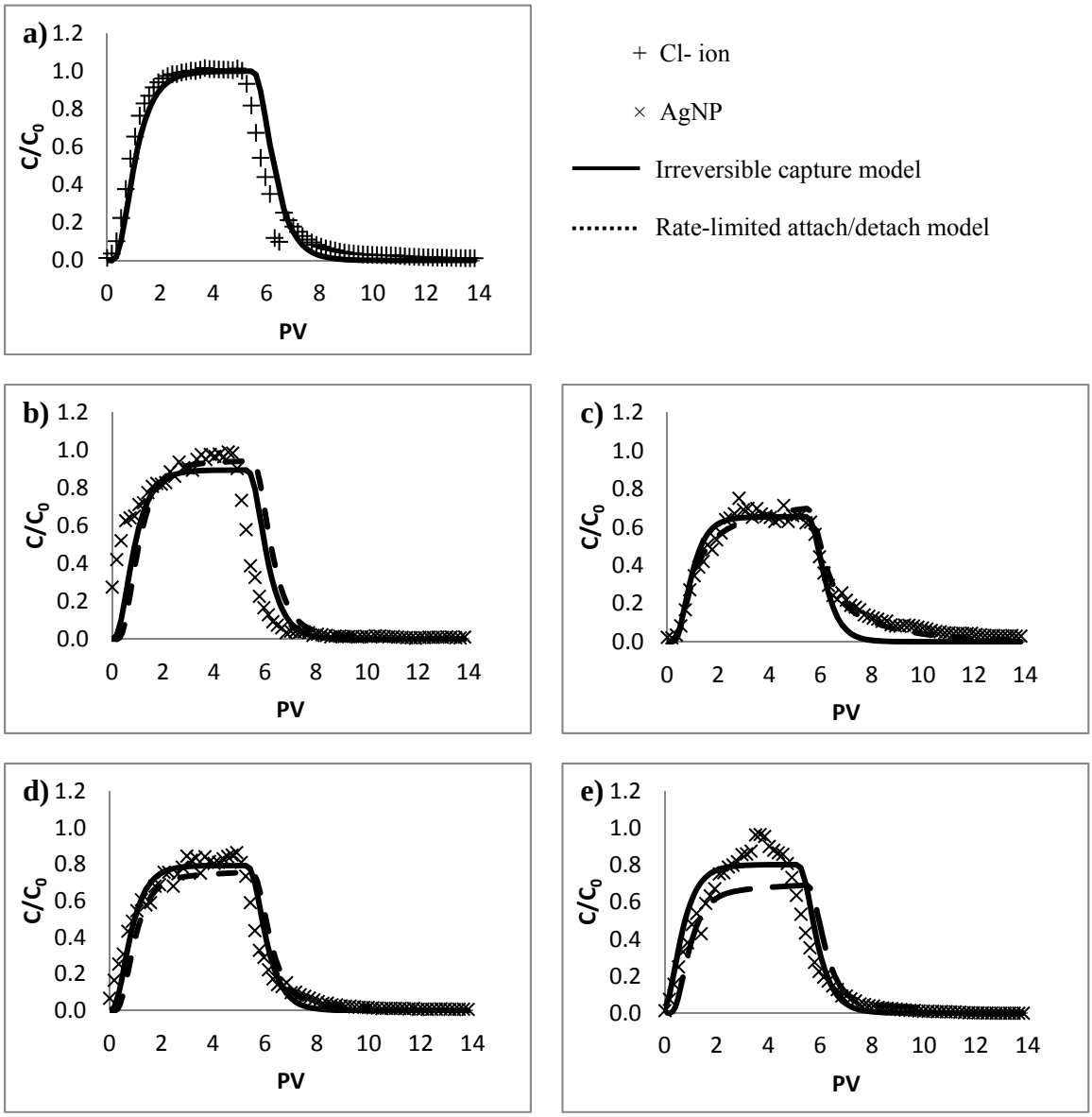


**Figure 4: Breakthrough curves for (a) Cl ion and AgNPs at (b) pH 4, (c) pH 6.5, (d) pH 9 and (e) pH 11, along with model fits. Experimental conditions: Cl ion: $C_0$ = 100 mg/L, AgNP: $C_0$ ~ 20 mg/L, ionic strength: 0.01 mM KCl and flow rate: 1 mL/min**

The Ag BTC at pH 4 showed a $C/C_0$ rise and elution similar to those for Cl ion (Figures 4a and b). At pH 4, metallic Ag dissociates into $Ag^+$ and $AgNO_3$ (as $HNO_3$ was added to adjust pH). There was no AgNP peak observed when effluent was measured by

UV spectrophotometer. A similar observation was reported for carbonate-coated AgNP at acidic pH (Piccapietra et al. 2011). The concentration of total Ag in the effluent increased with continuous introduction of Ag in 0.01 mM KCl at pH 4, until a maximum $C/C_0$ was reached after approximately 4.5 PV ($C/C_0 = 1$). After 60 minutes, the background electrolyte (0.01 mM KCl) was passed through the column to flush the Ag from the porous medium. More than 90% of the Ag was released from the column within approximately 10 PV. The release of deposited Ag (ion) is likely attributed to the elimination of the secondary energy minimum as discussed in previous studies using latex particles (Franchi and O'Melia 2003) and carbon nanotubes (Jaisi et al. 2008). The fact that the height of the BTC for Ag at pH 4 is smaller than the height of the tracer BTC may be due to attachment of Ag ions to negatively charged glass bead surfaces. He et al. (2009) provides indirect evidence for this phenomenon by observing that sand grains have a negatively charged surface at pH greater than 2, therefore by implication glass beads could be expected to exhibit similar properties.

Incomplete breakthrough at pH 6.5 (i.e., $C/C_0 < 1$) indicates the presence of a classical filtration mechanism such as direct interception. AgNPs exist in metallic form and less in the form of Ag ion at this pH, suggesting that electrical charge does not play as great a role in particle mobility or attachment. A tailing effect was observed while flushing the column with background solution (Figure 4c). A similar tailing was seen in experiments by Liu et al. (2009) using boron nanoparticles, in which the tailing effect was attributed to weak attachment of nanoparticles to collector surfaces. Filtration theory predicts that particles deposited on collector surfaces through the second energy minima

are susceptible to detachment by drag forces (Liu et al., 2009), which would explain tailing of the BTC during flushing of the column with background solution.

In the case of AgNP at pH 9 and 11, the maximum $C/C_0$ was greater than at pH 6.5 (Figure 4d and e). This finding is supported by Lin et al. (2011), in which AgNPs in glass beads showed greater attachment efficiency at lower pH. Incomplete breakthrough ($C/C_0 < 1$) is expected, similarly to the case of pH 6.5, due to classical filtration capture mechanisms.

Four basic mechanisms are considered to account for the capture of particles by grains of porous media: direct interception, convective diffusion, inertial impaction and gravitational deposition (Clark 2009). Gravitational deposition is only relevant in cases where flow velocity is small relative to settling velocity, or very low flow conditions (Clark 2009), and can therefore be ruled out as a factor in these experiments. Inertial impaction is primarily a function of the Stokes number, or ratio of stopping distance (inertia of particle) to collector (grain) size (Clark 2009). Since flow rate was held constant (1 mL/min) for each of these experiments, inertial impaction cannot be said to have any significant effect on the differences in breakthrough curves between different experiment runs. In convective diffusion, attachment efficiency is inversely proportional to the two-thirds power of particle size for a spherical collector such as a glass bead (Clark 2009), which means that, as particle size decreases, convective diffusion capture increases. We have seen the reverse trend in these experiments, i.e., as particle size increases, capture increases. This observation leads us to direct interception, which is directly proportional to the square of particle size (Clark 2009). Since, in these

experiments, attachment efficiency increases with increasing particle size (Table 1), we can deduce that direct interception is the dominant filtration mechanism at work.

**Table 1: Comparison of hydrodynamic size of AgNP, measured via DLS, versus height of BTC**

| pH | Average NP size (nm) | Maximum $C/C_0$ |
|---|---|---|
| 6.5 | 37.6 | 0.85 |
| 9 | 36.7 | 0.87 |
| 11 | 28.6 | 0.97 |

***Model Simulations of AgNP Transport***

The nonreactive chloride tracer test (Figure 4a) was simulated using Equation 5 with $T_p = 5.249$ and $Da^I_{irrev} = 0$ to obtain the value of $Pe$. A value of $Pe = 6.25$ was used to fit the chloride breakthrough data.

To simulate AgNP transport shown in Figures 4b, c, d and e, the Peclet number obtained from the chloride tracer test was used ($Pe = 6.25$). Model fits were obtained assuming either irreversible capture (Equation 5) or reversible attachment/detachment (Equations 6 and 7). Parameters for both models are given in Table 2. The method of moments for a sorbing and degrading solute (Pang et al. 2003) was applied to obtain values for $\frac{k_f}{\alpha}$ and $Da^I_{irrev}$, and for the reversible attachment/detachment model, $Da^I_{rev}$ was chosen to fit the tailing portion of the breakthrough curve. Figure 4b shows AgNP breakthrough data and model fits for experiments conducted at pH 4. Note that for the irreversible capture model, there is only one fitting parameter, $Da^I_{irrev}$ and for the reversible attachment/detachment model, there are only two parameters, $Da^I_{irrev}$ and

$Da^{I}_{rev}$. The small number of fitting parameters may explain the somewhat poor fits of the models to the rising and falling legs of the breakthrough data, especially as seen in Figure 4b. It would appear that either the flow rates or the input pulse times varied from experiment to experiment, resulting in the model simulations not closely matching the rising and falling legs of the breakthrough data. Note in all four figures (Figures 4b, c, d and e) that the shape of the data is simulated quite well by the reversible attachment/detachment model. In particular, the reversible attachment/detachment model appears to do an excellent job simulating the pH 6.5 BTC data (Figure 4c), and it is at this pH that attachment of the AgNPs is most significant, per the earlier discussion.

**Table 2: Model parameter values**

| | Irreversible Capture Model | | | Reversible Attachment/Detachment Model | | | |
|---|---|---|---|---|---|---|---|
| pH | Pe | R | $Da^{I}_{irrev}$ | Pe | R | $Da^{I}_{irrev}$ | $Da^{I}_{rev}$ |
| 4 | 6.25 | 1 | 0.097 | 6.25 | 1.593 | 0.01 | 0.10 |
| 6.5 | " | " | 0.39 | " | " | 0.28 | 0.60 |
| 9 | " | " | 0.21 | " | " | 0.20 | 0.15 |
| 11 | " | " | 0.20 | " | " | 0.28 | 0.20 |

To obtain mass balance, an additional column experiment at pH 6.5 was conducted. Total Ag was measured from effluent solution as well as from the porous medium. Expressed as fractions of the total mass of Ag input, 92% was recovered in the effluent, 3% was recovered from the porous medium, with the remaining 5% unaccounted for.

**Significance**

In this study, we examined the transport of AgNPs and Ag ions in porous media under saturated conditions at different pH. At low pH, silver was almost totally in the ionic form, and although transport of the Ag ion was similar to transport of a nonreactive tracer, Ag elution was incomplete ($C/C_0 < 1$), potentially due to attachment of Ag ions to negatively charged glass bead surfaces. On the other hand, AgNP transport was not retarded compared to Ag ion or tracer transport and its $C/C_0$ reached ~ 0.8. At high pH, AgNPs showed limited attachment efficiency, while at neutral pH, comparatively higher attachment efficiency was seen, as well as a tailing effect in the BTC, which implies that AgNP release into a near-neutral aquifer could result in a relatively long-term contamination issue. The understanding gained through this study will help in managing the disposal of AgNPs and their products, such as Ag ion. More research is needed in the study of AgNPs' and their products' fate and transport in the presence of cations, anions, organic matter and contaminants (organic, inorganic and heavy metals) in soil and groundwater.

Based on the modeling results shown in Figure 4 and the parameter values in Table 2, we can make a few observations:

1. Capture of AgNPs at low pH values (e.g., 4) is much less than at higher pH. Under acidic conditions, AgNPs are oxidized to produce ionic silver (Weinberg et al. 2011), which would be expected to resist attachment to collector surfaces, being smaller in size and therefore less likely to experience classical filtration capture mechanisms, compared to AgNPs.

2. Capture and tailing behavior is most significant at near-neutral pH. In a neutral pH environment, the oxidation described above is less likely to occur, so a higher rate of attachment is expected. Tailing may be caused by detachment from collector surfaces due to drag forces (Liu et al. 2009).
3. A model that incorporates both irreversible and reversible attachment is needed to simulate AgNP breakthrough data. In particular, a reversible attachment model is required to simulate breakthrough curve tailing at long times.

**Acknowledgements**

This research was supported by Air Force Medical Support Agency's Research and Development Division (AFMSA/SGRS), Department of Defense Funding Document No. F1ATD41003G004. Authors acknowledge Dr. Daniel Felker for training student in ICP analysis and gratefully acknowledge the technical assistance efforts of undergraduate students Nicole Jacques and Chelsea Riegel. This work was performed while Dr. Sushil R. Kanel was in the National Research Council Fellowship Program at the Air Force Institute of Technology, Wright Patterson Air Force Base, OH.

**Disclaimer**

The views expressed in this paper are those of the authors and do not reflect the official policy or position of the United States Air Force, The Department of Defense, or the United States Government.

## Bibliography

The references of this article are combined with the thesis.

# III. Conclusion

## Summary of Findings

In this study, the transport of AgNPs and Ag ions in porous media under saturated conditions at different pH was examined. At low pH, silver was almost totally in the ionic form and, although transport of Ag ion was similar to transport of a nonreactive tracer, Ag elution was incomplete ($C/C_0 < 1$), potentially due to attachment of Ag ions to negatively charged glass bead surfaces. AgNP transport was not retarded compared to Ag ion or tracer transport and its $C/C_0$ reached ~ 0.8. At high pH, AgNPs showed limited attachment efficiency, while at neutral pH, comparatively higher attachment efficiency was seen, as well as a tailing effect in the BTC, which implies that AgNP release into a near-neutral aquifer could result in a relatively long-term contamination issue. The understanding gained through this study will help in managing the disposal of AgNPs and their products, such as Ag ion.

The following three key observations were made:

1. Capture of AgNPs at low pH values (e.g., 4) is much less than at higher pH. Under acidic conditions, AgNPs are oxidized to produce ionic silver (Weinberg et al. 2011), which would be expected to resist attachment to collector surfaces, being smaller in size and therefore less likely to experience classical filtration capture mechanisms, compared to AgNPs.
2. Capture and tailing behavior is most significant at near-neutral pH. In a neutral pH environment, the oxidation described above is less likely to occur, so a higher

rate of attachment is expected. Tailing may be caused by detachment from collector surfaces due to drag forces (Liu et al. 2009).

3. A model that incorporates both irreversible and reversible attachment is needed to simulate AgNP breakthrough data. In particular, a reversible attachment model is required to simulate breakthrough curve tailing at long times.

**Recommendations for Future Research**

It is essential that bioenvironmental engineering officers in particular, and the Air Force and Department of Defense (DoD) in general, develop expertise with respect to the fate, transport, and effects of NMs, as NM use within the Air Force and DoD is anticipated to increase extensively in the coming years. NMs are currently being monitored as emerging contaminants of interest on DoD's Materials of Evolving Regulatory Interest Team (MERIT) watch list. In response to a Government Accountability Office query, the DoD noted a number of potential uses of NMs within DoD, a sampling of which follows: adaptive structures; responsive coatings; thermal control and system protection; nanoenergetics for munitions, fuels and high energy-density power generation and storage; sensors; signal processors.

Future study should investigate the effect on transport of variations in factors such as AgNP size, water flow rate, porous media grain size and AgNP surface modification. These are the objectives of Phase II of this study, to be conducted at AFIT in the coming year. Furthermore, research examining mitigation methods that can be applied to reduce

the potential for AgNPs to be transported to receptors at concentrations that may pose a risk would be valuable.

## Bibliography


Aitken, R. J., Chaudhry, M. Q., Boxall, A. B. A., and Hull, M. (2006). "Manufacture and Use of Nanomaterials: Current Status in the UK and Global Trends." Occupational Medicine-Oxford, 56, 300-306.

Amendola, V., Polizzi, S., and Meneghetti, M. (2007). "Free Silver Nanoparticles Synthesized by Laser Ablation in Organic Solvents and Their Easy Functionalization." Langmuir, 23(12), 6766-6770.

Aruguete, D. M., and Hochella, M. F. (2010). "Bacteria-Nanoparticle Interactions and Their Environmental Implications." Environmental Chemistry, 7(1), 3-9.

AshaRani, P. V., Low, K. M., Hande, M. P., and Valiyaveettil, S. (2009). "Cytotoxicity and Genotoxicity of Silver Nanoparticles in Human Cells." ACS Nano, 3(2), 279-290.

Benn, T., Cavanagh, B., Hristovski, K., Posner, J. D., and Westerhoff, P. (2010). "The Release of Nanosilver from Consumer Products Used in the Home." Journal of Environmental Quality, 39, 1875-1882.

Benn, T. M., and Westerhoff, P. (2008). "Nanoparticle Silver Released into Water from Commercially Available Sock Fabrics." Environmental Science & Technology, 42(11), 4133-4139.

Chen, X., and Schluesener, H. J. (2008). "Nanosilver: A Nanoproduct in Medical Application." Toxicology Letters, 176(1), 1-12.

Choi, O., Clevenger, T. E., Deng, B., Surampalli, R. Y., Ross Jr., L., and Hu, Z. (2009). "Role of Sulfide and Ligand Strength in Controlling Nanosilver Toxicity." Water Research, 43(7), 1879-1886.

Choi, O., Yu, C.-P., Esteban Fernandez, G., Hu, Z., and Choi, O. (2010). "Interactions of Nanosilver with Escherichia Coli Cells in Planktonic and Biofilm Cultures." Water Research, 44(20), 6095-6103.

Clark, Mark M. *Transport Modeling for Environmental Engineers and Scientists*. Hoboken, NJ: John Wiley & Sons, Inc., 2009.

Cumberland, S. A., and Lead, J. R. (2009). "Particle Size Distributions of Silver Nanoparticles at Environmentally Relevant Conditions." Journal of Chromatography, 1216, 9099-9105.

El Badawy, A. M., Luxton, T. P., Silva, R. G., Scheckel, K. G., Suidan, M. T., and Tolaymat, T. M. (2010). "Impact of Environmental Conditions (pH, Ionic Strength, and Electrolyte Type) on the Surface Charge and Aggregation of Silver Nanoparticles Suspensions." Environmental Science & Technology, 44(4), 1260-1266.

El Badawy, A. M., Silva, R. G., Morris, B., Scheckel, K. G., Suidan, M. T., and Tolaymat, T. M. (2011). "Surface Charge-Dependent Toxicity of Silver Nanoparticles." Environmental Science & Technology, 45, 283-287.

Fan, C. H., Chen, Y. C., Ma, H. W., and Wang, G. S. (2010). "Comparative Study of Multimedia Models Applied to the Risk Assessment of Soil and Groundwater Contamination Sites in Taiwan." Journal of Hazardous Materials, 182, 778-786.

Faunce, T., and Watal, A. (2010). "Nanosilver and Global Public Health: International Regulatory Issues." Nanomedicine, 5, 617-632.

Franchi, A., and O'Melia, C. R. (2003). "Effects of Natural Organic Matter and Solution Chemistry on the Deposition and Reentrainment of Colloids in Porous Media." Environmental Science & Technology, 37, 1122-1129.

Godinez, I. G., Darnault, C. J. G., and Godinez, I. G. (2011). "Aggregation and Transport of Nano-TiO2 in Saturated Porous Media: Effects of pH, Surfactants and Flow Velocity." Water Research, 45(2), 839-851.

He, F., Zhang, M., Qian, T., and Zhao, D. (2009). "Transport of Carboxymethyl Cellulose Stabilized Iron Nanoparticles in Porous Media: Column Experiments and Modeling." Journal of Colloid and Interface Science, 334, 96-102.

Huynh, K. A., and Chen, K. L. (2011). "Aggregation Kinetics of Citrate and Polyvinylpyrrolidone Coated Silver Nanoparticles in Monovalent and Divalent Electrolyte Solutions." Environmental Science & Technology.

Impellitteri, C. A., Tolaymat, T. M., and Scheckel, K. G. (2009). "The Speciation of Silver Nanoparticles in Antimicrobial Fabric Before and After Exposure to a Hypochlorite/Detergent Solution." Journal of Environmental Quality, 38, 1528-1530.

Jaisi, D. P., Saleh, N. B., Blake, R. E., and Elimelech, M. (2008). "Transport of Single-Walled Carbon Nanotubes in Porous Media: Filtration Mechanisms and Reversibility." Environmental Science & Technology, 42, 8317-8323.

Johnson, W. P., Li, X., and Yal, G. (2007). "Colloid Retention in Porous Media: Mechanistic Confirmation of Wedging and Retention in Zones of Flow Stagnation." Environmental Science & Technology, 41(4), 1279-1287.

Kanel, S. R., and Al-Abed, S. R. (2011). "Influence of pH on the Transport of Nanoscale Zinc Oxide in Saturated Porous Media." Journal of Nanoparticle Research, 13, 4035-4047.

Kanel, S. R., and Choi, H. (2007). "Transport Characteristics of Surface-Modified Nanoscale Zero-Valent Iron in Porous Media." Water Science and Technology, 55, 157-162.

Kanel, S. R., Goswami, R. R., Clement, T. P., Barnett, M. O., and Zhao, D. (2008). "Two Dimensional Transport Characteristics of Surface Stabilized Zero-Valent Iron Nanoparticles in Porous Media." Environmental Science & Technology, 42, 896-900.

Kanel, S. R., Nepal, D., Manning, B., and Choi, H. (2007). "Transport of Surface-Modified Iron Nanoparticle in Porous Media and Application to Arsenic(III) Remediation." Journal of Nanoparticle Research, 9, 725-735.

Kennedy, A. J., Hull, M. S., Bednar, A. J., Goss, J. D., Gunter, J. C., Bouldin, J. L., Vikesland, P. J., Steevens, J. A., and Kennedy, A. J. (2010). "Fractionating Nanosilver: Importance for Determining Toxicity to Aquatic Test Organisms." Environmental Science & Technology, 44(24), 9571-9577.

Khlebtsov, B., and Khlebtsov, N. (2011). "On the Measurement of Gold Nanoparticle Sizes by the Dynamic Light Scattering Method." Colloid Journal, 73, 118-127.

Kim, J. S., Kuk, E., Yu, K. N., Kim, J. H., Park, S. J., Lee, H. J., Kim, S. H., Park, Y. K., Park, Y. H., Hwang, C. Y., Kim, Y. K., Lee, Y. S., Jeong, D. H., and Cho, M. H. (2007). "Antimicrobial Effects of Silver Nanoparticles." Nanomedicine-Nanotechnology Biology and Medicine, 3, 95-101.

Kim, S., Choi, J. E., Choi, J., Chung, K.-H., Park, K., Yi, J., and Ryu, D.-Y. (2009). "Oxidative Stress-Dependent Toxicity of Silver Nanoparticles in Human Hepatoma Cells." Toxicology in Vitro, 23(6), 1076-1084.

Kim, Y. S., Kim, J. S., Cho, H. S., Rha, D. S., Kim, J. M., Park, J. D., Choi, B. S., Lim, R., Chang, H. K., Chung, Y. H., Kwon, I. H., Jeong, J., Han, B. S., and Yu, I. J. (2008). "Twenty-Eight-Day Oral Toxicity, Genotoxicity, and Gender-Related Tissue Distribution of Silver Nanoparticles in Sprague-Dawley Rats." Inhalation Toxicology, 20(6), 575-583.

Klaine, S. J., Alvarez, P. J. J., Batley, G. E., Fernandes, T. F., Handy, R. D., Lyon, D. Y., Mahendra, S., McLaughlin, M. J., and Lead, J. R. (2008). "Nanomaterials in the Environment: Behavior, Fate, Bioavailability, and Effects." Environmental Toxicology and Chemistry, 27(9), 1825-1851.

Kobayashi, M., Juillerat, F., Galletto, P., Bowen, P., and Borkovec, M. (2005). "Aggregation and Charging of Colloidal Silica Particles: Effect of Particle Size." Langmuir, 21, 5761-5769.

Kuhnen, F., Barmettler, K., Bhattacharjee, S., Elimelech, M., and Kretzschmar, R. (2000). "Transport of Iron Oxide Colloids in Packed Quartz Sand Media: Monolayer and Multilayer Deposition." Journal of Colloid and Interface Science, 231, 32-41.

Lerner, R. N., Lu, Q., Zeng, H., and Liu, Y. (2011). "The Effects of Biofilm on the Transport of Stabilized Zerovalent Iron Nanoparticles in Saturated Porous Media." Water Research, 46, 975.

Levard, C., Reinsch, B. C., Michel, F. M., Oumahi, C., Lowry, G. V., and Brown Jr., G. E. (2011). "Sulfidation Processes of PVP-Coated Silver Nanoparticles in Aqueous Solution: Impact on Dissolution Rate." Environmental Science & Technology, 45, 5260-5266.

Li, X., Lenhart, J. J., and Walker, H. W. (2010). "Dissolution-Accompanied Aggregation Kinetics of Silver Nanoparticles." Langmuir, 26(22), 16690-16698.

Lin, S., Cheng, Y., Bobcombe, Y., Jones, K. L., Liu, J., and Wiesner, M. R. (2011). "Deposition of Silver Nanoparticles in Geochemically Heterogeneous Porous Media: Predicting Affinity from Surface Composition Analysis." Environmental Science & Technology, 45(12), 5209-5215.

Liu, X., Wazne, M., Christodoulatos, C., and Jasinkiewicz, K. L. (2009). "Aggregation and Deposition Behavior of Boron Nanoparticles in Porous Media." Journal of Colloid and Interface Science, 330, 90-96.

Liu, J., and Hurt, R. H. (2010). "Ion Release Kinetics and Particle Persistence in Aqueous Nano-Silver Colloids." Environmental Science & Technology, 44(6), 2169-2175.

Liu, J., Sonshine, D. A., Shervani, S., and Hurt, R. H. (2010). "Controlled Release of Biologically Active Silver from Nanosilver Surfaces." ACS Nano, 4(11), 6903-6913.

Navarro, E., Baun, A., Behra, R., Hartmann, N. B., Filser, J., Miao, A.-J., Quigg, A., Santschi, P. H., and Sigg, L. (2008). "Environmental Behavior and Ecotoxicity of Engineered Nanoparticles to Algae, Plants, and Fungi." Ecotoxicology, 17(5), 372-386.

Nel, A., Xia, T., Mädler, L., and Li, N. (2006). "Toxic Potential of Materials at the Nanolevel." Science, 311, 622-627.

Nelson, K. E., and Ginn, T. R. (2011). "New Collector Efficiency Equation for Colloid Filtration in Both Natural and Engineered Flow Conditions." Water Resources Research, 47(5).

Nowack, B., and Bucheli, T. D. (2007). "Occurrence, Behavior and Effects of Nanoparticles in the Environment." Environmental Pollution, 150(1), 5-22.

Nowack, B., Krug, H. F., and Height, M. (2011). "120 Years of Nanosilver History: Implications for Policy Makers." Environmental Science & Technology.

Pang, L. P., Goltz, M., and Close, M. (2003). "Application of the Method of Temporal Moments to Interpret Solute Transport with Sorption and Degradation." Journal of Contaminant Hydrology, 60, 123-134.

Petosa, A. R., Brennan, S. J., Rajput, F., and Tufenkji, N. (2012). "Transport of Two Metal Oxide Nanoparticles in Saturated Granular Porous Media: Role of Water Chemistry and Particle Coating." Water Research, 46, 1273.

Piccapietra, F., Sigg, L., and Behra, R. (2011). "Colloidal Stability of Carbonate-Coated Silver Nanoparticles in Synthetic and Natural Freshwater." Environmental Science & Technology.

Ryan, J. N., and Elimelech, M. (1996). "Colloid Mobilization and Transport in Groundwater." Colloids and Surfaces: Physicochemical and Engineering Aspects, 107, 1-56.

Schrand, A. M., Rahman, M. F., Hussain, S. M., Schlager, J. J., Smith, D. A., and Syed, A. F. (2010). "Metal-Based Nanoparticles and Their Toxicity Assessment." WIREs Nanomedicine and Nanobiotechnology, 2, 544-568.

Shaw, B. J., and Handy, R. D. (2011). "Physiological Effects of Nanoparticles on Fish: A Comparison of Nanometals Versus Metal Ions." Environment International.

Solovitch, N., Labille, J., Rose, J., Chaurand, P., Borschneck, D., Wiesner, M. R., and Bottero, J.-Y. (2010). "Concurrent Aggregation and Deposition of TiO(2) Nanoparticles in a Sandy Porous Media." Environmental Science & Technology, 44, 4897-4902.

Song, J. E., Phenrat, T., Marinakos, S., Xiao, Y., Liu, J., Wiesner, M. R., Tilton, R. D., and Lowry, G. V. (2011). "Hydrophobic Interactions Increase Attachment of Gum Arabic- and PVP-Coated Ag Nanoparticles to Hydrophobic Surfaces." Environmental Science & Technology, 45, 5988-5995.

Tian, Y. A., Gao, B., Silvera-Batista, C., and Ziegler, K. J. (2010). "Transport of Engineered Nanoparticles in Saturated Porous Media." Journal of Nanoparticle Research, 12(7), 2371-2380.

Tolaymat, T. M., El Badawy, A. M., Genaidy, A., Scheckel, K. G., Luxton, T. P., and Suidan, M. (2010). "An Evidence-Based Environmental Perspective of Manufactured Silver Nanoparticle in Syntheses and Applications: A Systematic Review and Critical Appraisal of Peer-Reviewed Scientific Papers." Science of the Total Environment, 408(5), 999-1006.

Tufenkji, N., and Elimelech, M. (2004). "Correlation Equation for Predicting Single-Collector Efficiency in Physicochemical Filtration in Saturated Porous Media." Environmental Science & Technology, 38, 529-536.

USEPA. *Emerging Contaminants Nanomaterials Fact Sheet*. USEPA, 2010.

USEPA. http://water.epa.gov/ Accessed 15 February 2012.

Valocchi, A. J., and Werth, C. J. (2004). "Web-Based Interactive Simulation of Groundwater Pollutant Fate and Transport." Computer Applications in Engineering Education, 12, 75-83.

Weinberg, H., Galyean, A., Leopold, M., and Weinberg, H. (2011). "Evaluating Engineered Nanoparticles in Natural Waters." Trends in Analytical Chemistry, 30(1), 72-83.

Wijnhoven, S. W. P., Peijnenburg, W., Herberts, C. A., Hagens, W. I., Oomen, A. G., Heugens, E. H. W., Roszek, B., Bisschops, J., Gosens, I., Van de Meent, D., Dekkers, S., De Jong, W. H., Van Zijverden, M., Sips, A., and Geertsma, R. E. (2009). "Nano-Silver: A Review of Available Data and Knowledge Gaps in Human and Environmental Risk Assessment." Nanotoxicology, 3(2), 109-138.

Yang, Z., Liu, Z. W., Allaker, R. P., Reip, P., Oxford, J., Ahmad, Z., and Ren, G. (2010). "A Review of Nanoparticle Functionality and Toxicity on the Central Nervous System." Journal of the Royal Society Interface, 7, S411-S422.

Zhang, W., Yao, Y., Li, K., Huang, Y., and Chen, Y. (2011). "Influence of Dissolved Oxygen on Aggregation Kinetics of Citrate-Coated Silver Nanoparticles." Environmental Pollution, 159, 3757-3762.

# REPORT DOCUMENTATION PAGE

*Form Approved*
*OMB No. 074-0188*



**PLEASE DO NOT RETURN YOUR FORM TO THE ABOVE ADDRESS.**

| 1. REPORT DATE *(DD-MM-YYYY)* | 2. REPORT TYPE | 3. DATES COVERED *(From – To)* |
|---|---|---|
| Mar 2012 | Master's Thesis | Oct 10 –Mar 12 |

4. TITLE AND SUBTITLE

Influence of pH on the Transport of Silver Nanoparticles in Saturated Porous Media: Laboratory Experiments and Modeling

5a. CONTRACT NUMBER

5b. GRANT NUMBER

5c. PROGRAM ELEMENT NUMBER

6. AUTHOR(S)

Flory, Jason R., Captain, USAF

5d. PROJECT NUMBER
JON #11V247

5e. TASK NUMBER

5f. WORK UNIT NUMBER

7. PERFORMING ORGANIZATION NAMES(S) AND ADDRESS(S)

Air Force Institute of Technology
Graduate School of Engineering and Management (AFIT/EN)
2950 Hobson Way
WPAFB OH 45433-7765

8. PERFORMING ORGANIZATION REPORT NUMBER

AFIT/GIH/ENV/12-M02

9. SPONSORING/MONITORING AGENCY NAME(S) AND ADDRESS(ES)

AF Clinical Investigations Program, Office of the Air Force Surgeon General
Directorate for Modernization
Nereyda Sevilla, MPH, CAsP, PMP, CIV, HSO/Aerospace Physiologist
5201 Leesburg Pike, Suite 1501, Falls Church, VA 22041
Phone: 703-681-6383 (DSN: 761), Nereyda.sevilla@pentagon.af.mil

10. SPONSOR/MONITOR'S ACRONYM(S)
AFMSA/SG9S

11. SPONSOR/MONITOR'S REPORT NUMBER(S)

12. DISTRIBUTION/AVAILABILITY STATEMENT

APPROVED FOR PUBLIC RELEASE; DISTRIBUTION IS UNLIMITED.

13. SUPPLEMENTARY NOTES

This material is declared a work of the U.S. Government and is not subject to copyright protection in the United States.

14. ABSTRACT

Given the ubiquity of silver nanoparticles (AgNPs), the largest and fastest growing category of nanomaterials, and their potential for toxic effects to both humans and the environment, it is important to understand their environmental fate and transport. The purpose of this study is to gain information on the transport properties of unmodified AgNP suspensions in a glass bead-packed column under saturated flow conditions at different solution pH levels. Commercial AgNPs were characterized using high resolution transmission spectroscopy (HRTEM), dynamic light scattering (DLS) and ultraviolet (UV) visible spectroscopy. Transport data were collected at different pH levels (4, 6.5 and 9) at fixed ionic strength. Capture of AgNPs increased as the pH of the solution increased from 4 to 6.5. Further increase in pH to 9 decreased the attachment of AgNPs to the glass beads. AgNP concentration versus time breakthrough data were simulated using an advection-dispersion model incorporating both irreversible and reversible attachment. In particular, a reversible attachment model is required to simulate breakthrough curve tailing at near neutral pH, when attachment is most significant.

15. SUBJECT TERMS

Silver nanoparticles, nanomaterials, fate and transport, advection-dispersion model

| 16. SECURITY CLASSIFICATION OF: | | | 17. LIMITATION OF ABSTRACT | 18. NUMBER OF PAGES | 19a. NAME OF RESPONSIBLE PERSON |
|---|---|---|---|---|---|
| a. REPORT | b. ABSTRACT | c.THIS PAGE | UU | 53 | LEEANN RACZ, Maj, USAF, BSC, PhD, PE |
| U | U | U | | | 19b. TELEPHONE NUMBER *(Include area code)* (937) 255-6565, x 2259 (leeann.racz@afit.edu) |

Standard Form 298 (Rev. 8-98)
Prescribed by ANSI Std. Z39-18